

# Estimation of Site Response in Time Domain Using the Meyer–Yamada Wavelet Analysis

by Gülüm Birgören and Kojiro Irikura

**Abstract** In most applications of the stochastic Green's function simulation, amplitude characteristics of seismic responses at target sites are taken into consideration, but phase information of them is often disregarded or just assumed to be random. However, when seismic waves from the source pass through different geological strata, they take multiple paths and, as result, the arrival times of different seismic phases to the receiver vary. Especially in basin structures, seismic waves trapped in unconsolidated deposits or secondarily induced at the basin edges elongate the duration of ground motion. In the present study, a simple empirical method using the Meyer–Yamada wavelet procedure is proposed for the phase-dependent site response estimation in time domain. The method reveals the amplitude and phase effects of extended duration of ground motion on site response by utilizing the wavelet transform. Because the wavelet transform yields a localization of a signal in both frequency and time domains, the phase information of the signal stays intact. Application of this method has been performed using the aftershock records of the 1999 Düzce, Turkey Earthquake ( $M_w$  7.1). Amplitude spectra of absolute site responses were also calculated by a spectral calculation method at each station for comparison purpose. Good agreement between the amplitude spectra calculated with the wavelet method and those of the spectral calculation method supports the efficiency of the proposed method.

## Introduction

Conventional methods for estimating the site response are mainly based on the calculation of the amplitude spectrum of the ground motion and do not effectively reflect the information about the duration (Borcherdt, 1970; Andrews, 1986; Iwata and Irikura, 1988; Fletcher and Boatwright, 1991). However, in sedimentary basins the impact of wave propagation effects on ground motion can be more significant than that due to the surficial layers. The long-period ground motions recorded at the sites underlain by deep basins may be associated not with the direct body waves but with secondarily generated surface waves, which elongates the ground motion. These long-period surface waves can cause large amount of damage in flexible structures. Therefore, extended duration of the ground motion is an inevitable consequence of the wave generation in sedimentary-filled basin structures and has to be considered together with site amplification for realistic simulation of the ground motion for assessment of a future earthquake.

Arrival time information of seismic waves to a site is kept in the phase spectrum of a signal. Derivation of the unwrapped phase spectrum gives the group delay time versus frequency behavior of the site. Sawada (1998) has suggested that the group delay time calculation is an efficient

method to understand the phase property of the seismic motion. Following the method of Sawada (1998), Beavual *et al.* (2003) showed the variety of the lengthening of the ground motion at basin stations using observed and simulated data. They attempted to estimate synthetic signals at stations located inside a basin by modifying the amplitude and phase spectra of the signal at a reference site. However, this method demands very close distance between the reference site and the sites of interest such that the source and path effects cancel out.

The method presented here focuses on the calculation of the site response at basin stations, taking into consideration the elongation of the ground motion due to basin effects, and proposes an empirical method to estimate the phase-dependent site response directly in the time domain utilizing the Meyer–Yamada wavelet analysis. Because the method estimates the site response at a station directly from its time domain data by removing source and path effects at each wavelet level, the phase information is automatically kept in the analysis; therefore, the method necessitates neither a near-distant reference site nor additional analyses to estimate the elongation of ground motion.

The 1999 Turkey earthquakes (17 August,  $M_w$  7.4 and

12 November,  $M_w$  7.1) caused extensive damage, in particular, in Düzce City and several towns located in the Düzce Basin. To perform a realistic ground-motion simulation to understand the nonuniform damage distribution in the basin, site amplification and extended duration of the ground motion due to basin-generated waves should be computed. To achieve this objective the proposed method was applied to the aftershock data set of the 1999 Düzce, Turkey, earthquake.

## Time Domain Representation of Site Response

### Discrete Wavelet Transform

Because it has been used for several decades, a nonstationary signal can be treated as the combination of cosine and sine waves, which comprises the basis of the Fourier analysis. The signal can be more accurately characterized by the usage of basis functions, in other words, wavelets (Daubechies, 1990; Mallat, 1989; Meyer 1989). The wavelet transform decomposes a signal into its high- and low-frequency components by using shifted and scaled versions of the mother wavelet. Orthogonality is the most desired property in any signal analysis. Besides, localization or compactness of the wavelet is required to avoid the redundancy of the signal. Hence, in most of wavelet transform applications in seismology, the discrete wavelet analysis is preferred because the wavelet function of the discrete wavelet analysis satisfies the orthonormality condition (Meyer, 1989). A time series  $f(t)$  can be represented by an inverse discrete wavelet transform as

$$f(t) = \sum_j \sum_k \alpha_{j,k} \Psi_{j,k}(t) \quad (1)$$

$\Psi_{j,k}(t)$  represents the analyzing wavelet (basis function),  $t$  is the time,  $j$  and  $k$  are the integer values denoting the spatial scale and position of the wavelet, respectively (Yamada and Ohkitani, 1991). Wavelet coefficients ( $\alpha_{j,k}$ ) are calculated by convolving the time series by the analyzing wavelet as

$$\alpha_{j,k} = \int_{-\infty}^{\infty} \Psi_{j,k}(t) * f(t) dt \quad (2)$$

Asterisk denotes the complex conjugate.

The analyzing wavelet is derived by translation and dilatation from a mother wavelet function ( $\Psi$ ) as following;

$$\Psi_{j,k}(t) = 2^{j/2} \Psi(2^j t - k) \quad (3)$$

Because wavelet transform is a linear technique wavelet coefficients are modified in the time domain even though they are associated with frequency levels (wavelet levels). In other words, data operations can be performed with wavelet coefficients of the corresponding frequency band instead of the signal itself. Hence, this property of the transform allows

the user to modify the signal in each frequency band. Inverse wavelet transform reassembles the signal from modified coefficients.

For a discrete time series  $f(t)$  with sampling rate  $\Delta t$  and the number of data points  $N$  ( $N = 2^n$  where  $n$  is an integer) inverse discrete wavelet transform is defined as (Yamada and Ohkitani, 1991);

$$f(t) = \sum_{j=0}^{N-1} \sum_{k=0}^{2^j-1} \alpha_{j,k} \Psi_{j,k}(t). \quad (4)$$

Among several analyzing wavelet definitions, the Meyer–Yamada procedure (Meyer, 1989; Yamada and Ohkitani, 1991) has been employed in the present study (Fig. 1). The priority of the Meyer–Yamada wavelet is that amplitudes of the wavelet spectrum approximately correspond to the amplitudes of the power spectrum of a signal at the  $j$ th scale.

$$E_j = \sum_k |\alpha_{j,k}|^2 \quad (5)$$

Frequency range of the  $j$ th scale is defined as

$$\frac{2^j}{3Td} \leq f \leq \frac{2^{j+2}}{3Td} \quad (6)$$

$Td$  is the signal length in seconds ( $Td = N \Delta t$ ). Note that the Meyer–Yamada Wavelet is nonzero only between the frequency ranges given at (6). Wavelet coefficients have high resolution in time and low resolution in frequency as the wavelet level increases and vice versa. The wavelet decompositions of a strong-motion accelerogram and its power and wavelet amplitude spectra are illustrated in Figure 2 as an example.

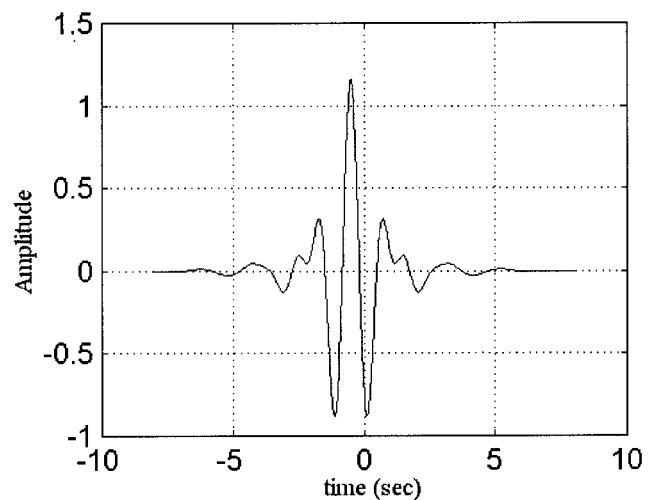


Figure 1. Meyer mother wavelet in the time domain.

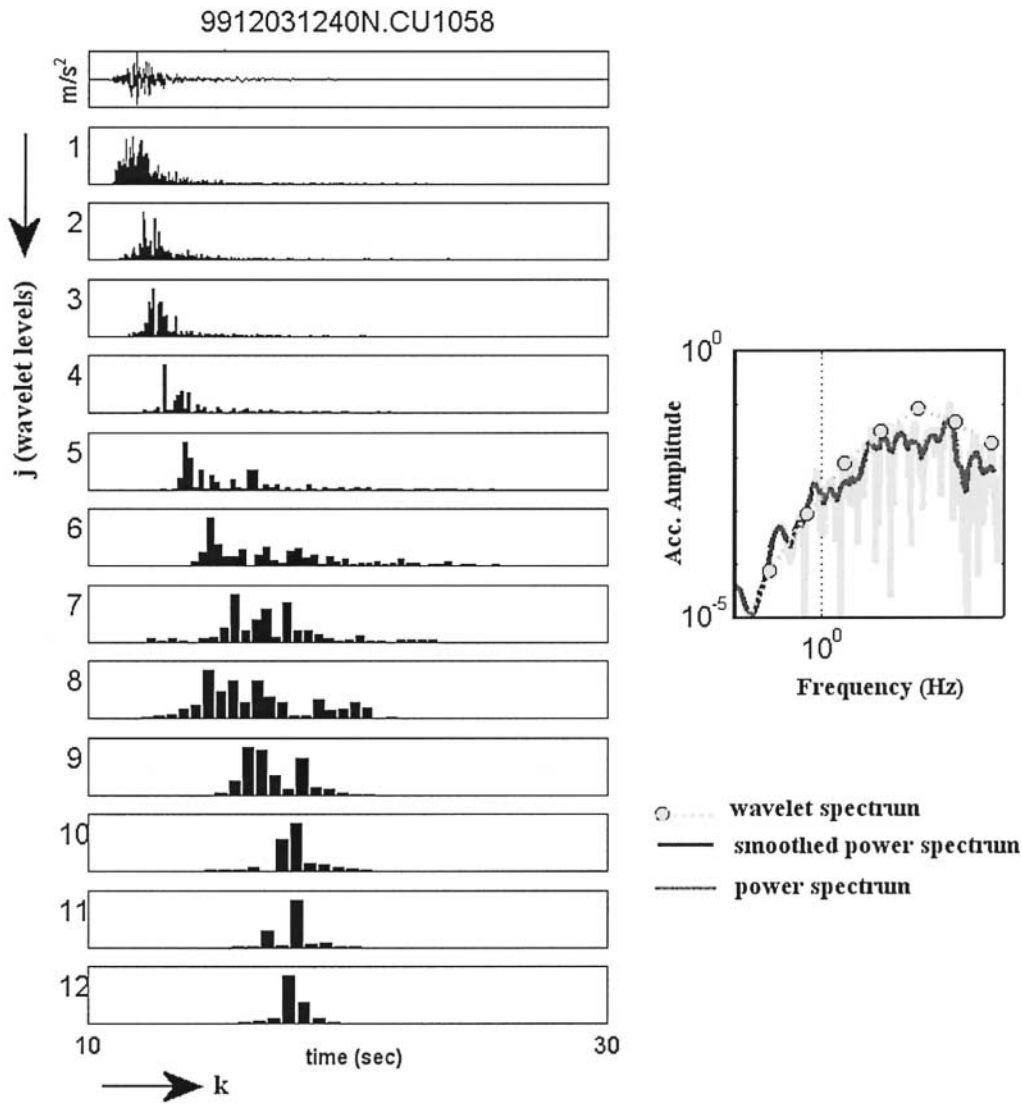


Figure 2. (left) Wavelet decompositions of a strong-motion accelerogram. (right) Power spectrum of the same accelerogram is shown in light gray. Amplitudes of each wavelet level (each frequency band) are drawn at geometric mean frequencies  $(2^{j+1}/3T_d)$  with filled circles. Thick black line represents 20% logarithmic smoothing of the power spectrum.

Site Response Calculation with Wavelet Method

The Fourier amplitude spectrum of an observed seismic signal is represented as the multiplication of source, propagation path, and site response (Iwata and Irikura, 1988).

$$O_{ij}(f) = S(f)_i P(f)_{ij} G(f)_j \tag{7}$$

where  $S(f)_i$  is the seismic source of the  $i$ th event,  $P(f)_{ij}$  is the propagation path effect from the  $i$ th event to the  $j$ th site, and  $G(f)_j$  is the site response at the  $j$ th site.

The simplest empirical way to calculate local site responses is to remove the source and propagation path effects from the observed record by taking the spectral ratio between the site of interest and a reference site for the same

event, as proposed by Borchardt (1970). This method is effective if the distance between the stations is much smaller than the hypocentral distance.

The empirical estimation of the site response in time domain is performed essentially in the same way as the site amplification is calculated from the spectral ratio technique. This method utilizes the discrete wavelet transform to localize a seismic signal in both time and frequency domains simultaneously and enables retention of amplitude and phase properties of the observed signal. The method is based on the modification of wavelet coefficients of seismic signals at each discrete wavelet level to yield wavelet coefficients of site response. In the method each horizontal component of the seismic signal, starting from  $S$ -wave onset to the end of the data, is decomposed into its wavelet levels, wavelet

coefficients at each level are divided by the corresponding source and propagation factors as follows:

$$\alpha_{j,k,i}^G = \frac{\alpha_{j,k,i}^O}{|S(\omega)_{j,i}| |P(\omega)_{j,i}|} \quad (8)$$

( $\alpha_{j,k,i}^G$ ) and  $\alpha_{j,k,i}^O$  are the wavelet coefficients of the site response and the wavelet coefficients of the signal at the  $j$ th scale of the  $i$ th event. The denominators  $S(\omega)_{j,i}$  and  $P(\omega)_{j,i}$  in (8) are the source and propagation path scalar terms at the geometric mean frequency ( $2^{j+1}/3Td$ ) at the  $j$ th scale of the  $i$ th event, respectively. In the calculation, the wavelet scales whose frequency range is smaller than the noise levels of signals are suppressed by forcing the related coefficients to zero (i.e.,  $\alpha_{j,k,i} = 0$ ). Schematic illustration of the calculation method is given in Figure 3.

The source spectrum required in (7) and consequently in (8) is calculated from the estimation of the low-frequency flat level ( $\Omega$ ) and corner frequency ( $f_c$ ) of the displacement spectra with  $w^2$  point source assumption at reference stations (Aki, 1967; Brune, 1970).

$$S(f)_i = \frac{\Omega_i/2}{1 + \left(\frac{f}{f_{ci}}\right)^2} \quad (9)$$

where  $f$  is the frequency. Flat level is divided by 2 to account for the free surface effect. Regarding propagation path ef-

fects, radiation of  $S$  waves from the source are taken into account. Propagation path effect has a general equation as

$$P(f)_{ij} = \frac{1}{R_{ij}} e^{-\pi R_{ij} f / Q(f) V_s} \quad (10)$$

where  $R$  is the hypocentral distance between the  $i$ th event and the  $j$ th station,  $Q(f)$  is the quality factor, and  $V_s$  is the  $S$ -wave velocity of the medium.

Equation (8) is valid for the small earthquakes in short distance with similar source durations. If this condition is fulfilled, phase delay due to the source effect and the propagation path effects can be assumed negligibly small compared with those due to the site effects. Finally, the average coefficients of the site response at a station are calculated as

$$\alpha_{j,k}^G = \sum_{i=1}^n \frac{\alpha_{j,k,i}^G}{n} \quad (11)$$

where  $\alpha_{ji} \neq 0$ ,  $n = \{\text{number of events whose } \alpha_{j,k,i} \neq 0\}$ .

The modified average wavelet coefficients calculated from the preceding operations together with wavelet function yields the site response in the time domain through the inverse wavelet transform defined in (4). According to the mean value theorem of statistics, the noise should disappear as the number of records used in the analysis increases. Thus, the stacking technique in (11) enhances common site effects (coherent part) and reduces noises (incoherent part).

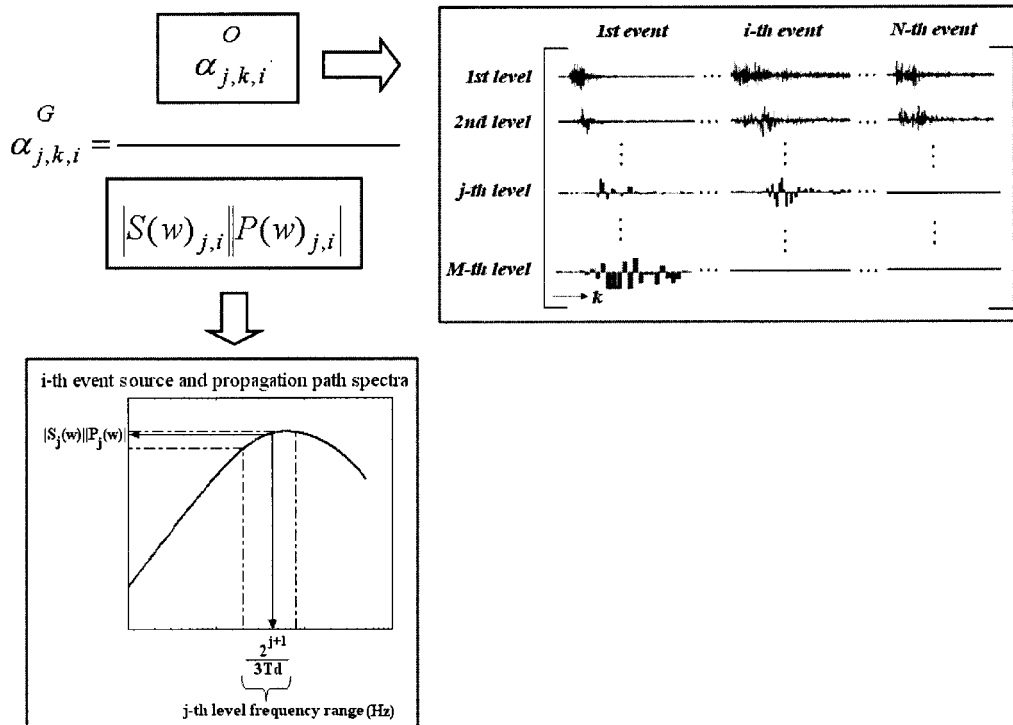


Figure 3. Schematic representation of the site response in the time domain by the wavelet method.

Probably one of the most important priorities of the wavelet analysis over the Fourier analysis is that it can yield time and frequency information simultaneously in accordance with the uncertainty principle, where the Fourier analysis can yield only the frequency information. Current analysis can also be done in the complex domain, because it does not explicitly use the time-frequency calculation. However, Fourier coefficients are not stable for each event recorded at a station and the smoothing functions used for the analysis do not always guarantee the orthonormality condition. In addition, wavelet analysis makes it possible to explain the amplitudes with a limited number of positions rather than using all data points.

Spectral Calculation Method (SCM) with Reference Event

Absolute site-amplification factors are estimated by a spectral method to evaluate the validity of the site-amplification calculation with the wavelet method.

The site-amplification factors are calculated by removing the source and propagation path effects from the observed record. A diversion from the technique of Borchardt (1970) arises from the fact that, the source spectra, estimated for the events recorded at the reference site, and propagation path spectra of all events are calculated empirically according to (9) and (10) as long as the source spectra are explained with the  $w^2$  model. Therefore, the absolute site effects can be estimated at each station with respect to the theoretical  $S(f)$  and  $P(f)$  spectra.

The definition of average site response at the  $j$ th station calculated for  $N$  events is expressed as:

$$G_j(f) = \sum_{i=1}^N \frac{O_j(f)}{S_i(f)P_{ij}(f)} / N \quad (12)$$

In Figure 4 the calculation method is expressed in a schematic way. The calculation method will be addressed as

“the spectral calculation method (SCM) with reference event,” hereafter.

A Case of Düzce Basin

During the 1999 Kocaeli and Düzce earthquakes, urban areas located in the Düzce Basin, in particular, Düzce and Kaynaşlı, suffered from heavy structural damage. The damage is mainly associated with the malfunction of the structural system as well as the effect of the soil characteristics. Borings drilled up to 15 m and seismic refraction measurements performed in Düzce City and Kaynaşlı Town show similar characteristics. The areas underlain by the Quaternary deposit consists of silt, clay, and sandy gravels. The groundwater levels estimated from borehole logs vary between 2 and 7 m (Kayabalı *et al.*, 2001; Özdemir *et al.*, 2002). A microtremor study carried out by Kudo *et al.* (2002) in Düzce City indicates that Düzce is a sedimentary basin with 1.5 km depth, consisting of thick and soft sediments at surface ( $V_s \sim 260$  m/sec) and intermediate depths ( $V_s \sim 460\text{--}510$  m/sec).

The site responses at the observation stations inside and outside of the Düzce Basin were analyzed by using the strong-motion accelerograms of the 1999 Düzce, Turkey, earthquake aftershocks, recorded by temporary networks deployed by Kandilli Observatory and Earthquake Research Institute of Boğaziçi University (EQE) and LDEO of Columbia University (CU). The strong-motion stations are listed in Table 1. Fourteen shallow earthquakes of duration magnitude,  $3.2 \leq M_d \leq 5.0$  with hypocentral distance of up to 40 km were used. For the estimation of site-amplification factors, the station CU1058 was chosen as the reference site based on the topographic and geological data.

Figure 5 shows the location of the stations and aftershocks together with the bandpass-filtered (0.5–2.0 Hz) velocity waveforms of north–south component of the aftershock no. 12, starting from  $P$ -wave arrival. Even though the recording time is shorter in the basin stations due to misadjustment of instruments, the ground-motion differences

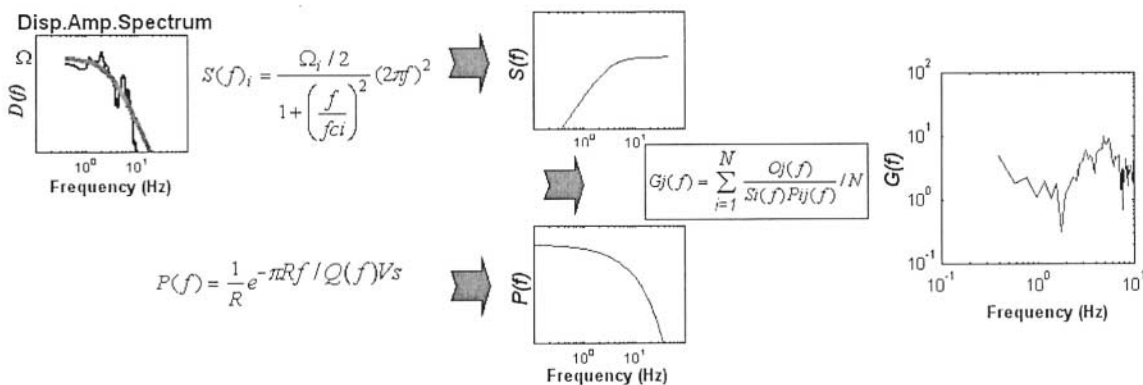


Figure 4. Schematic representation of the calculation method of site amplification by the spectral calculation method with reference event (SCM).

Table 1  
Strong-Motion Recording Stations and Their Specifications

Station Name	Location	Instrument Specifications
CU1058	40.75N–31.06E	
CU1059	40.75N–30.87E	
CU1060	40.78N–30.63E	Reftek-72A-08 24 bit
CU1061	40.72N–30.79E	Terra T 320
CU1062	40.72N–30.82E	(full scale $\pm 2$ g)
CU0362	40.67N–30.67E	S.R: 100 Hz*
CU0375	40.74N–30.87E	
CU0531	40.70N–30.85E	
EQESAZ	40.84N–31.05E	Kinometrics SSA 12 (full scale $\pm 0.5$ g) S.R: 200 Hz
EQEBAL	40.78N–31.10E	GeoSys GSR-12
EQEGON	40.82N–31.21E	Terra T 320
EQEFCM	40.83N–31.19E	(full scale $\pm 2.0$ g) S.R: 200 Hz

\*S.R., sampling rate.

between basin stations and the reference station are quite visible. The waveforms get complicated inside the basin and strong-motion durations get longer. The extended duration of shaking at basin stations may be the indicator of the basin-induced surface waves.

Noise-amplitude spectra of the records were calculated by using the 5-sec time window before  $P$ -wave arrival. Records having signal-to-noise ratios lower than a factor of 2 were removed from the analysis. At most CU stations the signal-to-noise ratio is above the factor of 2 between 0.4 and 10 Hz. Most of the records at the EQEGON and EQEFCM stations either have very short duration before  $P$ -wave arrival or started after  $P$ -wave onset. Therefore, the noise levels of those earthquakes are biased at lower-frequency ranges, (particularly at  $f \leq 0.5$  Hz) Acceleration spectra were calculated for a 5-sec window of the records, starting 1 sec before the  $S$ -wave arrival, as the horizontal vector summation of north–south and east–west component's spectra and transformed in displacement with double integration. Amplitudes were corrected for  $1/R$  geometric spreading,  $R$  is the hypocentral distance. The low-frequency flat level ( $\Omega$ ) and corner frequency ( $f_c$ ) of the displacement spectra of 14 earthquakes recorded at the reference site was estimated by a Genetic Algorithm (Holland, 1975) assuming  $w^2$  source model. The seismic-moment values ( $M_0$ ) were derived from

$$M_0 = 4\pi\rho V_s^3 \Omega/R_{\theta\phi} \quad (13)$$

$S$ -wave velocity of the medium ( $V_s$ ), density ( $\rho$ ), and radiation-pattern coefficient for  $S$  waves ( $R_{\theta\phi}$ ) are taken as 3.2 km/sec, 2.7 g/cm<sup>3</sup> (Mindevalli and Mitchell, 1989), and  $\sqrt{2/5}$  (Andrews, 1986), respectively. The source parameters of the 14 earthquakes were given in Table 2.

Moya (personal comm., 2003) estimated the quality factor of the Düzce area as  $Q = 154f^{0.15}$  through a spectral inversion method by using a larger aftershock data set recorded at the same stations. Propagation path spectra were calculated with equation (10), based on the  $Q$  value mentioned above.

Figure 6 shows the average site response results together with site response results of all individual earthquakes used in the calculation for the frequency range of 0.5–10 Hz. The data preparation for the calculation of phase-dependent site responses were done in the following order: All the records were corrected to zero baseline, cosine tapered starting from 1 sec before the  $S$ -wave onset until the end of data, and zero padded to equalize the number of wavelet levels of each earthquake at a station. Decomposition levels were chosen according to the noise level of records. In this aspect, the data selection differs from the SCM. For instance, the data having noise contamination beyond 0.7 Hz were not included in the estimation with the SCM; however, it can be included in the wavelet method suppressing the low-frequency level coefficients and including higher-frequency level coefficients in the estimation. The largest event ( $M_d 5$ ) was not used in the wavelet calculation to keep the source duration of events similar. Time domain representations of the site responses, bandpass filtered between 0.5 and 5 Hz, are drawn next to the stations in Figure 7. Low-frequency level is due to the reliability of the observed data. Average site response spectra of the stations calculated from both methods were compared in Figure 8. Note that the site response estimation with the SCM comprises mainly the  $S$ -wave portion of the data where the wavelet method covers all available waves arriving after  $S$ -wave onset.

## Results

Site response estimations using spectral calculation and wavelet methods are presented. Some of the remarkable points can be summarized as follows:

- Flat site amplification in low-frequency range and fundamental frequency observed in higher-frequency range at the station CU1058 imply harder soil site. This result supports the appropriateness of the reference site selection.
- Two close basin stations EQEFCM and EQEGON show similar response shape and amplification levels. The stations EQEBAL and EQESAZ located in the edge and center of the basin have amplification levels as high as 10 at about 2 Hz and 1 Hz, respectively. This is the largest site amplification level estimated for basin stations at mid-frequency range (0.5–2 Hz)
- Time domain representation of site response shown in Figure 7 reflects the difference in soil characteristics inside the basin and outside the basin. The stations located on harder soil (CU1058, CU1060) show a site response almost like an impulse function; however, stations inside the basin, in particular, EQEBAL and EQESAZ, exhibit longer and more complex response functions and are rich in high-frequency contents.
- At stations CU1059 and CU0375 the difference in amplification levels is significant even though they are located approximately 500 m from each other. The station CU0375 has the highest amplification levels with short

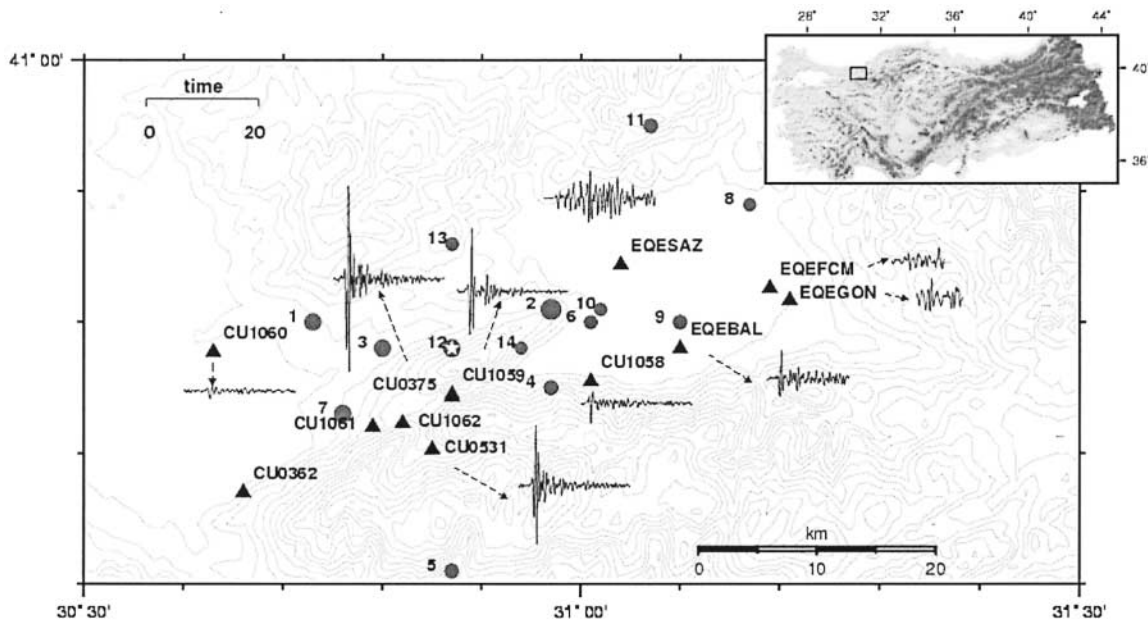


Figure 5. Location of the strong-motion stations (filled triangles) and aftershocks (filled circles). North–South component strong-motion velocity records of the earthquake no. 12 (99/12/20/03:27  $M_d$  4.2, depth = 10.0 km), bandpass filtered between 0.5 and 2 Hz are drawn next to the stations to show the variation of ground-motion records.

Table 2  
Source Parameters of Reference Events

No.	Event Date (yy/mm/dd/h:min)	Depth (km)	Moment (N m)	$f_c$ (Hz)	Magnitude ( $M_d$ )
1	99/11/19/14:01	10.0	3.9E15	1.7	4.1
2	99/11/19/19:59	9.0	2.6E16	0.9	5.0
3	99/11/21/04:31	10.0	6.0E15	1.6	4.2
4	99/11/21/04:33	7.0	4.8E14	2.1	3.5
5	99/12/03/12:40	5.0	3.5E15	2.1	3.7
6	99/12/03/12:46	3.0	4.4E14	2.3	3.3
7	99/12/13/19:13	7.0	5.7E15	1.2	4.3
8	99/12/14/17:38	8.0	5.2E14	1.9	3.6
9	99/12/15/00:12	8.0	3.6E14	2.4	3.3
10	99/12/17/05:29	8.0	2.4E14	2.5	3.2
11	99/12/17/12:12	3.5	4.5E14	2.2	3.5
12	99/12/20/03:27	10.0	4.3E15	2.3	4.2
13	99/12/20/03:41	7.0	6.1E14	4.1	3.4
14	99/12/23/14:40	5.0	5.0E14	4.5	3.2

duration. This reflects a strong velocity contrast between thin uppermost sedimentary layer and engineering basement layer under the station.

- The average site amplification spectra estimated by the wavelet analysis method show good agreement with the estimates obtained by the SCM.

### Conclusion and Discussion

An empirical method has been proposed to estimate the site response in time domain. The main asset of the method is that it allows the calculation of site response without ig-

noring the phase properties of a seismic signal. The method was applied to the aftershock data set of the 1999 Düzce Earthquake. The fairly good fitting of both amplitude levels and shape of the site response calculated with the SCM and the wavelet method supports the validity of the proposed method. The efficiency of the method should be tested with the stochastic Green’s function simulations and compared with the damage distribution observed at the Düzce Basin.

The success of the method highly depends on the existence of the reference site to define source effects with high accuracy. *S*-wave onset picking is also a major factor affecting results, because misalignment of records highly increases the error in estimation of phase information. Moreover, the method requires a high signal-to-noise ratio to calculate low-frequency site response realistically.

Probably the most important limitation of this approach is related to the calculation of source and propagation path spectra. The method can not be performed successfully without accurate estimation of the seismic moment, corner frequency of reference events, and inelastic attenuation factor of the medium. Azimuthal dependence of the site response was not considered in the present study because of limited number of the earthquakes. For further estimation this factor should be taken into consideration, in particular, for the basin edge stations.

Beside these, many extensions of this research still deserve further consideration; the main assumption followed in this research is that site response mainly consists of the coherent part of the signal (as in equation 11). Spectra fittings shown in the application confirm this assumption. A full development of the site response considering both co-

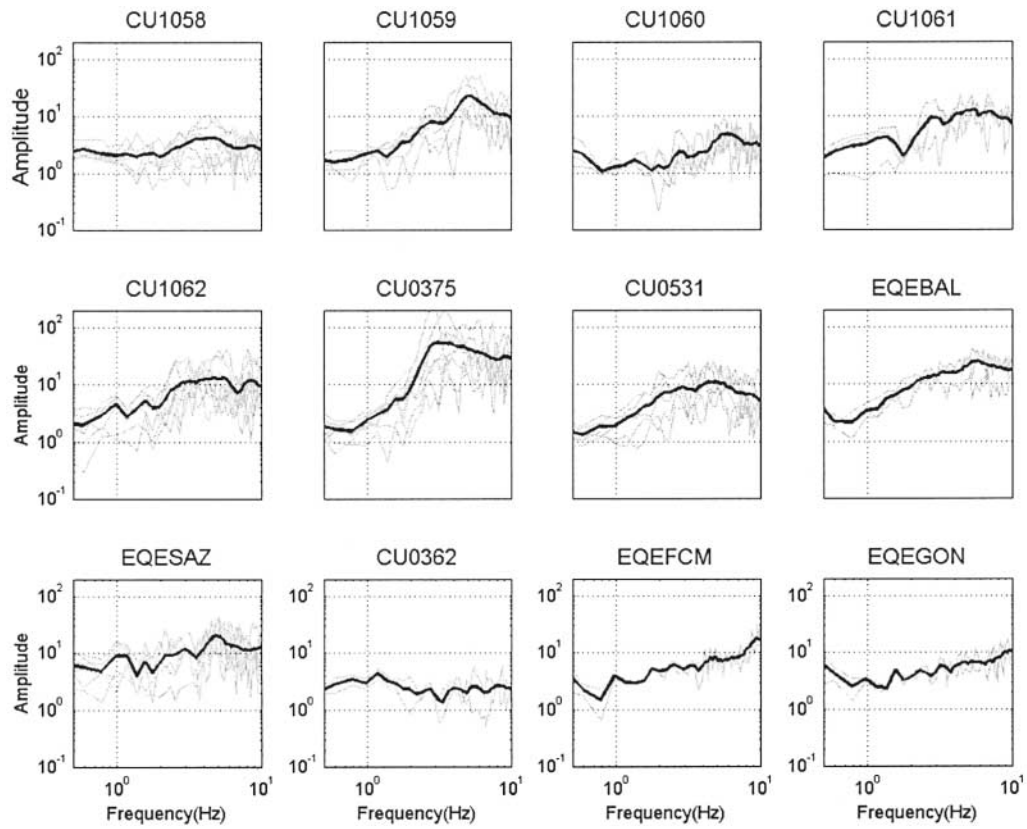


Figure 6. Average site response results versus frequency calculated with the spectral calculation method with reference event (SCM). Gray lines show the events used for calculation.

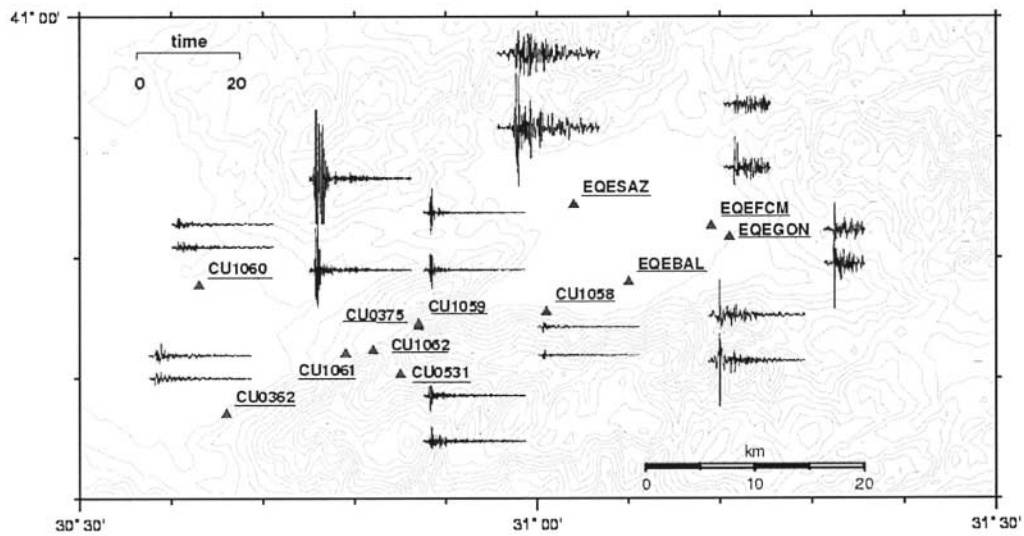


Figure 7. Time domain representations of the site response bandpass filtered between 0.5 and 5 Hz. Upper and lower waveforms are the north–south and east–west components of the site response at each station, respectively.

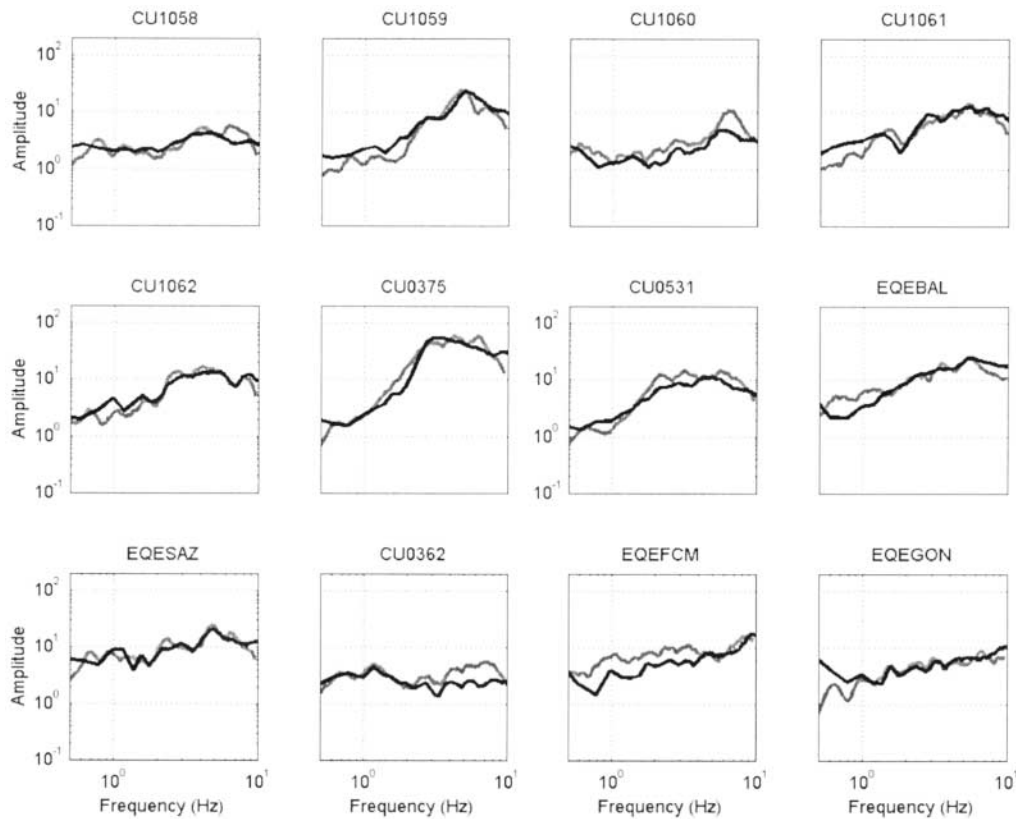


Figure 8. Comparison of amplitude spectra of site response calculated with spectral calculation (in black) and wavelet methods (in gray).

herent and incoherent parts of the signal is beyond the scope of the present study. For further direction of the research, the incoherent part of site effects should be calculated based on amplitude spectra, assuming random phases to prevent underestimation of the site response.

Another issue raised by the current results is the overestimation of the high-frequency ground motion inside the basin, possibly because of the nonlinear effect of the soil. The response of a specific site may change according to different deterministic scenarios under consideration. Special attention should be given to the nonlinearity of the soil in basin structures. For more realistic prediction of the ground motion, synthesized waveforms should be reanalyzed, considering nonlinear effects and assuming a shallow velocity structure model of the region.

### Acknowledgments

We thank Aaron Moya for the calculation of the frequency-dependent quality factor and for his help using the Generic Algorithm method. We also thank the scientists and technicians at the Boğaziçi University and Columbia University, who are in charge of the strong-motion stations whose recordings are used in the present study. This work was supported by the Special Project for Earthquake Disaster Mitigation in Urban Areas from the Ministry of Education, Culture, Sports, Science, and Technology of Japan. Some of the graphs were prepared by using GMT v3.1 (Wessel and Smith, 1998).

### References

- Aki, K. (1967). Scaling law of seismic spectrum, *J. Geophys. Res.* **72**, 1217–1231.
- Andrews, D. J. (1986). Objective determination of source parameters and similarity of earthquakes of different size, in *Earthquake Source Mechanics*, D. Shamita, J. Boatwright, and C. H. Scholtz (Editors), Vol. 6, American Geophysical Union, Washington, D.C., 259–267.
- Beavual, C. Y., P.-Y. Bard, P. Moczo, and J. Kristek, (2003). Quantification of frequency-dependent lengthening of seismic ground-motion duration due to local geology: applications to the Volvi area (Greece), *Bull. Seism. Soc. Am.* **93**, 371–385.
- Borcherdt, R. D. (1970). Effects of local geology on ground motions near San Francisco Bay, *Bull. Seism. Soc. Am.* **60**, 29–61.
- Brune, J. N. (1970). Tectonic stress and the spectra of seismic shear waves from earthquakes, *J. Geophys. Res.* **75**, 4997–5009.
- Daubechies, I. (1990). The wavelet transform, time-frequency localization and signal analysis, *IEEE Trans. Inf. Theory* **36**, no. 5, 961–1005.
- Fletcher, J., and J. Boatwright (1991). Source parameters of Loma Prieta aftershocks and wave propagation characteristics along the San Francisco peninsula from a joint inversion of digital seismograms, *Bull. Seism. Soc. Am.* **81**, 1783–1812.
- Holland, J. H. (1975). *Adaptation in Nature and Artificial Systems*, University of Michigan Press, Ann Arbor, Michigan.
- Iwata, T., and K. Irikura, 1988. Source parameters of the 1983 Japan Sea earthquake sequence, *J. Phys. Earth.* **36**, 155–184.
- Kayabali, K., E. Ulugergerli, and E. Tokgöz. (2001) Düzce İli Merkezinde 246 Hektarlık Alanın İmar Planına Esas Jeolojik-Jeofizik-Jeoteknik Etüd Raporu, Ankara (in Turkish).
- Kudo, K., T. Kanno, H. Okada, O. Özel, M. Erdik, T. Sasatani, S. Higashi, M. Takahashi, and K. Yoshida (2002). Site-specific issues for strong

- ground motions during the Kocaeli, Turkey, earthquake of 17 August 1999, as inferred from array observations of microtremors and aftershocks, *Bull. Seism. Soc. Am.* **92**, 448–465.
- Mallat, S. G. (1989). A theory for multiresolution signal decomposition: the wavelet representation, *IEEE Trans. Pattern Anal. Machine Intell.* **11**, no. 7, 674–693.
- Meyer, Y. (1989). Orthonormal wavelets, in *Wavelets*, J. M. Combes, A. Grossman, and Ph. Tchamitchian (Editors). Springer, Berlin.
- Mindevalli, O. Y., and B. J. Mitchell (1989). Crustal structure and possible anisotropy in Turkey from seismic surface wave dispersion, *Geophys. J. Int.* **98**, 93–106.
- Özdemir, P., B. Taşkın, C. Vatansever, A. Sezen, A. İlki, and H. Boduroğlu (2002). November 12, 1999 Düzce earthquake: a reconnaissance report for the town of Kaynaslı, in *12th Proc. European Conference of Earthquake Engineering*, London, United Kingdom.
- Sawada, S. (1998). Phase characteristics on the site amplification of layered ground with irregular interface, in *The Effect of Surface Geology on Seismic Motion*, K. Irikura, K. Kudo, H. Okada, and T. Sasatani (Editors), Balkema, Rotterdam, 1009–1013.
- Yamada, M., and K. Ohkitani (1991). Orthonormal wavelet analysis of turbulence, *Fluid Dyn. Res.* **8**, 101–115.
- Wessel, P., and W. H. F. Smith (1998). New, improved version of Generic Mapping Tools released, *EOS Trans. AGU* **79**, 579.
- K.O.E.R.I, Bogazici University  
Cengelkoy, Istanbul  
34684 Turkey  
birgore@boun.edu.tr  
(G.B.)
- D.P.R.I., Kyoto University  
Gokasho, Uji  
Kyoto, 611-0011, Japan  
irikura@egmdpri01.dpri.kyoto-u.ac.jp  
(K.I.)

Manuscript received 4 September 2003.